

A strongly interacting photonic quantum walk using single atom beam splitters

Xinyuan Zheng^{1,*} and Edo Waks^{1,2,3,†}

¹*Department of Electrical and Computer Engineering and Institute for Research in Electronics and Applied Physics, University of Maryland, College Park, Maryland 20742, USA*

²*Joint Quantum Institute, University of Maryland, College Park, Maryland 20742, USA*

³*Department of Physics, University of Maryland, College Park, Maryland 20742, USA*

(Dated: March 8, 2022)

Photonic quantum walks are powerful tools for quantum simulation. However, most theoretical and experimental works related to this topic have implemented quantum walks with linear optical elements, which lack photon-photon interactions. Here we theoretically show that an array of single atom beam splitters can implement a discrete-time photonic quantum walk with strong photon-photon interactions. We calculate the dynamics of this strongly interacting quantum walk for the case of two photons using quantum trajectory theory. We show that the photon correlation functions exhibit strong photon-photon interaction and that the statistical pattern of the quantum walk can be tuned by post-selecting the delays between photon detection events. Finally, we propose a practical realization of our quantum walk based on time-multiplexed synthetic dimensions. Our proposal presents a new approach for photonic quantum simulation with strongly interacting photons.

Photonics provides an efficient way to implement quantum walks, which play an important role in quantum simulation and quantum computation[1–6]. Photonic quantum walks can be realized using beam splitters[6–10] or coupled waveguide arrays[11–13] to simulate a wide range of Hamiltonians and implement quantum computing algorithms[1, 2, 5, 14]. In the linear optical regime, a two-photon quantum walk can simulate the dynamics of non-interacting bosons, fermions or anyons[7–10]. But in order to study strongly-correlated many-body physics, a strongly interacting photonic quantum walk with single-photon-level nonlinearities is required.

Photonic quantum walks with strong photon-photon interactions can be realized in both discrete and continuous-time. For continuous-time quantum walks, coupled cavity arrays containing superconducting quantum emitters offer a Jaynes-cummings Hubbard Hamiltonian that can support two polariton bound states similar to the Bose-Hubbard Hamiltonian[15–17]. For discrete-time quantum walks, some phenomenological nonlinearities have been proposed and studied[18–20], but we still lack physical systems that can realize these nonlinearities. A more realistic nonlinearity that has been demonstrated experimentally relies on a system composed of a two-level atom strongly coupled to a waveguide[21–26]. This system acts as a nonlinear beam splitter when multiple photons are incident upon it[21–23], and can potentially replace the linear beam splitters used in a discrete-time quantum walk. But leveraging this nonlinearity in a photonic quantum walk is largely unexplored, and the theoretical analysis of this system remains extremely complex.

Here we propose a strongly interacting discrete-time photonic quantum walk using single atom beam splitters. To analyze the system, we develop a formalism based on quantum trajectory theory to derive a direct solution to the output statistics of the walk[27, 28]. We calculate

the two-photon correlation functions for all pairs of output channels and show that they exhibit the signature of strong photon-photon interactions. Finally, we propose a practical realization of our quantum walk based on time-multiplexed synthetic dimensions[29–32]. Our proposal presents a new approach for quantum simulation using photons.

Before introducing the strongly interacting quantum walk, we first review the common approach of implementing a linear discrete-time photonic quantum walk illustrated in Figure 1a. This method uses a linear beam splitter array, also referred to as a quantum Galton board. At each step, the beam splitters direct the photons to the left or right with equal probabilities, generating a quantum walk. Figure 1a illustrates a special case where the photons start at position 0 and undergo a three-step quantum walk. Photon counters at the output channels of the final step, denoted by square brackets, detect the positions and directions of the output photons after they have undergone all steps. The detection statistic emerges as a result of interference between the many different paths the photons can take to reach their respective output ports. The linear Galton board has been extensively analyzed and experimentally demonstrated[7–10, 29, 33]. Although the linear Galton board can exhibit complex multi-photon interference effects, the linear optical elements in the Galton board cannot induce strong photon-photon interactions.

To introduce strong photon-photon interactions, we propose the nonlinear Galton board shown in Figure 1b. This Galton board is a feedforward network whose nodes are identical single atom beam splitters. Figure 1c shows the detailed structure of a single atom beam splitter consisting of a two-level atom strongly coupled to a waveguide as proposed in [21], with two inputs and two outputs. Alternatively, one can replace the two-level atom in Figure 2c with an atom-cavity system in the “fast cavity

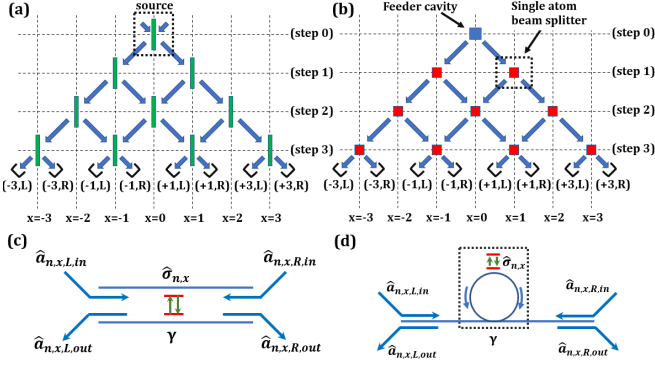


FIG. 1. (a) A three-step linear quantum walk. At each step, the linear beam splitters partition each walker to the left or right. The square brackets represent photon counters that detect the final positions and directions of the walkers. (b) The nonlinear Galton board consists of an array of single atom beam splitters. A feeder cavity at $(0,0)$ injects photons into the system. (c) A single atom beam splitter composed of a two-level system coupled to a waveguide. (d) An alternative implementation using an atom-cavity system in the “fast cavity regime” [34, 35] in place of the two-level system in (c).

regime” where we can adiabatically eliminate the cavity degree of freedom [34, 35], as shown in Figure 1d. In both cases, the input-output relations for the single atom beam splitter is:

$$\begin{aligned}\hat{a}_{n,x,R,out} &= \hat{a}_{n,x,L,in} + \sqrt{2\gamma}\hat{\sigma}_{n,x} \\ \hat{a}_{n,x,L,out} &= \hat{a}_{n,x,R,in} + \sqrt{2\gamma}\hat{\sigma}_{n,x}\end{aligned}\quad (1)$$

In the above equations, n and x label the step number and the horizontal position of the specific beam splitter. We denote the input modes from the left(L)/right(R) as $\hat{a}_{n,x,L/R,in}$ and the output modes towards the left(L)/right(R) as $\hat{a}_{n,x,L/R,out}$. $\hat{\sigma}_{n,x}$ is the lowering operator of the two-level system and the parameter γ characterizes its spontaneous emission rate into the waveguide. For a single quasi-monochromatic input photon, a single atom beam splitter behaves as a linear beam splitter [21]. The reflection and transmission coefficients are given by $r_\delta = \frac{-i\gamma}{i\gamma + \delta}$ and $t_\delta = \frac{\delta}{i\gamma + \delta}$ [21], where δ is the detuning between the atom and the input photon. However, the single atom beam splitter exhibits a strong nonlinearity when multiple photons are injected upon it. Even in the case of two photons, the scattering process can no longer be described by individual reflection and transmission coefficients. Instead, the atom induces strong photon-photon interactions giving rise to complex multi-photon scattering matrix elements [21–24].

To numerically analyze the output statistics of the nonlinear Galton board, we use a quantum trajectory theory approach, originally proposed by Carmichael [27, 28, 36] for the analysis of cascaded quantum systems. We utilize

a feeder cavity at position $(0,0)$ to inject quantum light into the system, as illustrated in Figure 1b. The feeder cavity has a decay rate κ , which determines the bandwidth of the injected photons. All the atoms have the same parameter γ . The parameter δ denotes the detuning between the feeder cavity and each individual atom. The quantum Galton board can now be viewed as a cascaded quantum system. Following the quantum trajectory theory formalism, we introduce the non-Hermitian Hamiltonian for the system (see supplementary section):

$$\begin{aligned}\hat{H} &= -2i(\kappa + i\delta)\hat{b}_{0,0}^\dagger\hat{b}_{0,0} - 2i\gamma\sum_{n,x}\hat{\sigma}_{n,x}^\dagger\hat{\sigma}_{n,x} \\ &- 2i\gamma\sum_{n,x}\hat{\sigma}_{n,x}^\dagger\left(\sum_{\substack{n'<n \\ |n-n'|=|x-x'|}}\hat{\sigma}_{n',x'}\right) - 2i\sqrt{\gamma\kappa}\sum_{n=1}^N(\hat{\sigma}_{n,-n}^\dagger + \hat{\sigma}_{n,n}^\dagger)\hat{b}_{0,0}\end{aligned}\quad (2)$$

where $1 \leq n \leq N$, $|x| \leq n$ and $x = n + 2k$ for any $\hat{\sigma}_{n,x}$. In the above Hamiltonian, $\hat{b}_{0,0}$ is the bosonic lowering operator for the feeder cavity. The photon counters monitor all the output modes at the last step, $\hat{a}_{N,x,d,out}$. By repeatedly applying equation 1 for $n = 1, 2, \dots, N$, we obtain the following relationship between $\hat{a}_{N,x,d,out}$ and the lowering operators $\hat{\sigma}_{n,x}$ (see supplementary section):

$$\begin{aligned}\hat{a}_{N,x,L,out} &= \sum_{n'=(x+N)/2}^N\sqrt{2\gamma}\hat{\sigma}_{n',x+N-n'} \\ \hat{a}_{N,x,R,out} &= \sum_{n'=(N-x)/2}^N\sqrt{2\gamma}\hat{\sigma}_{n',x+n'-N}\end{aligned}\quad (3)$$

The above equations hold only for $|x| \neq N$. The two output modes at the ends of the Galton board, $\hat{a}_{N,-N,L,out}$ and $\hat{a}_{N,N,R,out}$ have a slightly different form and are given by $\hat{a}_{N,-N,L,out} = \sqrt{2\kappa}\hat{b}_{0,0} + \sum_{n'=1}^N\sqrt{2\gamma}\hat{\sigma}_{n',-n'}$ and $\hat{a}_{N,N,R,out} = \sqrt{2\kappa}\hat{b}_{0,0} + \sum_{n'=1}^N\sqrt{2\gamma}\hat{\sigma}_{n',n'}$.

To start the quantum walk, we can set the feeder cavity into any initial state. Here we focus on the specific case of a two-photon Fock state $\frac{1}{\sqrt{2}}(\hat{b}_{0,0}^\dagger)^2|vac\rangle$. Following the quantum trajectory theory formalism, the complete output statistics of the nonlinear Galton board should be described by a collection of two-photon correlation functions [27, 28, 34]:

$$\begin{aligned}\Gamma_{x_2,d_2;x_1,d_1}(\tau,t) &= \\ \langle \hat{a}_{N,x_1,d_1,out}^\dagger(t)\hat{a}_{N,x_2,d_2,out}^\dagger(t+\tau)\hat{a}_{N,x_2,d_2,out}(t+\tau)\hat{a}_{N,x_1,d_1,out}(t) \rangle\end{aligned}\quad (4)$$

Equation 4 provides the time-ordered probability density function of collecting the first photon in the photon counter at position x_1 and direction $d_1 \in \{L,R\}$ at time t and the second photon in the photon counter located at x_2 and d_2 at time $t + \tau > t$. Using the correlation function in equation 4, we define the interval-time

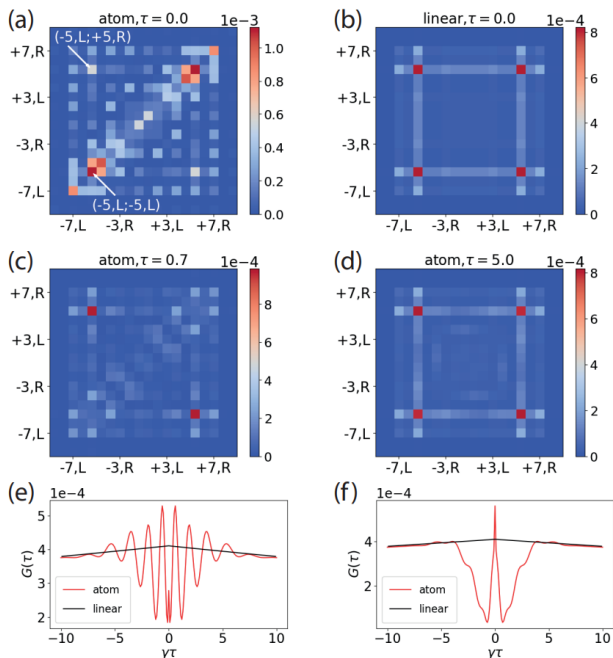


FIG. 2. Results for $\kappa \ll \delta = \gamma$. (a) The statistical pattern matrix for the nonlinear Galton board for $\tau = 0$, showing correlated statistics. (b) The statistical pattern for $\tau = 0$ for the linear Galton board. (c-d) The statistical pattern for the nonlinear Galton board for $\tau = 0.7, 5.0$, showing anti-correlated and uncorrelated statistics. (e) $G_{-5,L;+5,R}(\tau)$ and $G_{+5,R;-5,L}(-\tau)$, plotted for all $0 \leq \tau \leq 10$. (f) $G_{-5,L;-5,L}(|\tau|)$ for all $0 \leq \tau \leq 10$.

correlation, $G_{x_2,d_2;x_1,d_1}(\tau) = \int_0^\infty dt \Gamma_{x_2,d_2;x_1,d_1}(\tau, t)$ [34]. This function represents the time-ordered marginal probability of detecting the two photons with a time separation of τ , which is the quantity typically measured in a two-photon coincidence experiment. To average out over this time-ordering we define $\tilde{G}_{x_2,d_2;x_1,d_1}(\tau) = G_{x_2,d_2;x_1,d_1}(\tau) + G_{x_1,d_1;x_2,d_2}(\tau)$. By arranging the labels (x_i, d_i) in the same linear order as shown for the photon counters in Figure 1b and fixing τ , we can plot $\tilde{G}_{x_2,d_2;x_1,d_1}(\tau)$ as a $(2N+2) \times (2N+2)$ matrix. We refer to this matrix as the *statistical pattern*. It characterizes the output statistics of the quantum walk after post-selecting all two-photon detection events with a certain time interval τ regardless of time-ordering. Conversely, we may also fix a pair of channels $\{x_1, d_1; x_2, d_2\}$ and plot the curve $G_{x_2,d_2;x_1,d_1}(\tau)$ together with $G_{x_1,d_1;x_2,d_2}(\tau)$.

We first analyze the case where the single atom beam splitters act as nearly ideal 50/50 beam splitters for a single photon input. To achieve this condition, we set $\gamma = \delta = 1$, and select the feeder cavity decay rate to be $\kappa = 0.002$. This decay rate is sufficiently small to ensure that the input photon bandwidth is narrow and we are in the quasi-monochromatic limit. To illustrate the effects of interactions, we compare our results to that of a lin-

ear Galton board containing linear, dispersionless beam splitters in Figure 1a. Computationally, we replace the input-output relations in equation 1 with input-output relations of a linear beam splitter and carry out the same quantum trajectory theory procedure (see supplementary section).

Figure 2a shows the statistical pattern of the nonlinear Galton board after 9 steps for $\tau = 0$, corresponding to post-selecting near-simultaneous two-photon detections. The statistical pattern exhibits a strongly correlated behavior in which the two photons are more likely to be found in the same output channel. In comparison, Figure 2b shows the result for the linear Galton board for $\tau = 0$. Here the two walkers *independently* partition themselves to the left and right, with maximal detection probabilities at $(-5, L)$ and $(+5, R)$. The statistical pattern in Figure 2a is therefore a result of photon-photon interactions induced by the single atom beam splitters in the nonlinear Galton board.

Figure 2c plots the statistical pattern for the nonlinear Galton board for $\tau = 0.7$. This statistical pattern is drastically different from Figure 2a and exhibits anti-correlated statistics where the two walkers are found in two opposite output channels $(-5, L)$ and $(+5, R)$. By tuning τ we can therefore generate either correlated or anti-correlated statistics. Notably, in contrast to the τ -dependent statistical pattern for the nonlinear Galton board, the statistical pattern for the linear Galton board (Figure 2b) remains the same for *any* τ (see supplementary section). Finally, Figure 2d shows the case for $\tau = 5.0$. Here, the post-selected photon detection events are sufficiently separated in time such that we may treat the photons as scattering individually. Therefore, we recover the statistical pattern for the linear Galton board in Figure 2b.

To attain a better understanding of the varying statistical pattern, we select two representative channel pairs, as indicated in Figure 2a, and plot $G_{x_2,d_2;x_1,d_1}(\tau)$ together with $G_{x_1,d_1;x_2,d_2}(\tau)$ against τ . For the anti-correlated channel pair $\{-5, L; +5, R\}$, we observe an oscillation in $G(\tau)$ that gradually dies out for $\tau > 6$ as shown in Figure 2e. For the correlated channel pair $\{-5, L; -5, L\}$, we observe a narrow peak around $\tau = 0$ followed by a valley with minimal value at $\tau = 0.7$ (Figure 2f). In comparison, the correlation functions $G(\tau)$ for the linear Galton board are two identical smooth curves shown in black (Figure 2e, 2f), indicating no photon-photon interaction.

The nonlinear Galton board can also generate quantum walks with unequal splitting ratios by simply changing the detuning. As an instructive example, we analyze the case where the quasi-monochromatic input photons are resonant with the two-level atoms ($\delta = 0$). In this regime, the single atom beam splitter can reflect a single input photon with near unity efficiency. Figure 3a shows the statistical pattern for $\tau = 0$, while Figure 3b shows

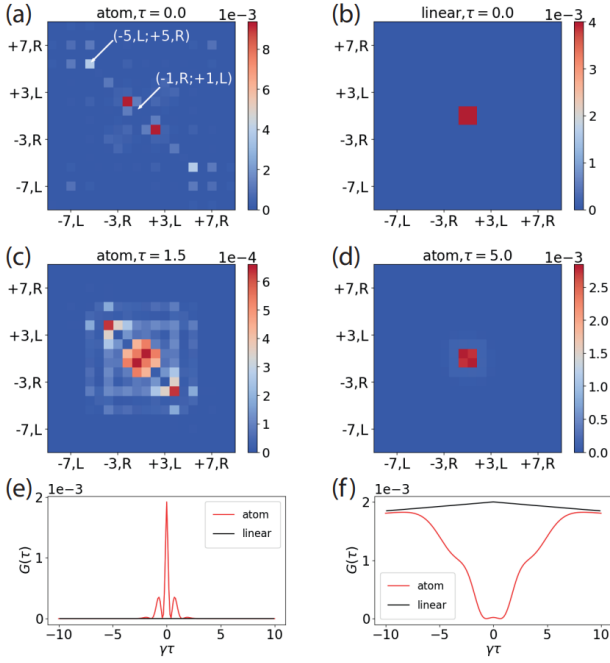


FIG. 3. Results for $\delta = 0$, $\kappa \ll \gamma$. (a) The statistical pattern matrix for the nonlinear Galton board for $\tau = 0$, showing anti-correlated statistics excluding the center. (b) The statistical pattern for $\tau = 0$ for the linear Galton board. (c-d) The statistical pattern for the nonlinear Galton board for $\tau = 1.5, 5.0$, converging to the pattern in (b) as τ increases. (e) $G_{-5,L;+5,R}(\tau)$ and $G_{+5,R;-5,L}(-\tau)$, plotted for all $0 \leq \tau \leq 10$. (f) $G_{-1,R;+1,L}(\tau)$ and $G_{+1,L;-1,R}(-\tau)$ for all $0 \leq \tau \leq 10$.

the result for the linear Galton board. For the linear Galton board, the photons are trapped at the center since they reflect back and forth repeatedly between adjacent beam splitters around the center ($x = 0$). Surprisingly, the nonlinear Galton board exhibits a drastically different statistical pattern that predominantly excludes the center (Figure 3a). Instead, local maximums appear on the anti-correlated diagonal of the statistical pattern matrix, indicating two-photon detections in opposite output channels, $(-x, L)$ and $(+x, R)$. At $\tau = 1.5$ (Figure 3c) this anti-correlated statistical pattern gradually shrinks, while at $\tau = 5.0$ it becomes almost identical to the linear case (Figure 3d).

Similarly, we pick two pairs of representative output channels indicated in Figure 3a and plot the correlation functions against τ . For the nonlinear Galton board, the correlation function for the anti-correlated channel pair $\{-5, L; +5, R\}$ exhibits a high peak around $\tau = 0$ as shown in Figure 3e. For some other anti-correlated channel pairs, similar two-photon correlation functions can be observed (see supplementary section). In contrast, for the center channel pair $\{+1, L; -1, R\}$ (Figure 3f), the photon correlation function exhibits a deep valley with minimum

0 around $\tau = 0$. The drastic difference between the correlation functions of the linear (black) and nonlinear (red) quantum walks is again the result of strong photon-photon interactions.

Having analyzed the properties of the nonlinear Galton board, we next consider potential experimental realizations. We propose an implementation using time-multiplexed synthetic dimensions [29–32] to avoid the need to fabricate large arrays of single atom beam splitters. Figure 4 shows an implementation of the linear Galton board using this method, which requires only one beam splitter coupled to two feedback loops with different time delays, $T_0 + T_x$ and $T_0 - T_x$. Photons are injected into the system via the two input ports and photon counters at the output ports detect the photons. The same beam splitter at different time delays $nT_0 + xT_x$ acts as different beam splitters in the Galton board, provided that the pulse width d of the photons satisfies $d \ll v_g T_x$ and $T_x \ll T_0$ [29]. All the photon counters in Figure 1a are represented by the two photon counters in Figure 4a at different time delays [29].

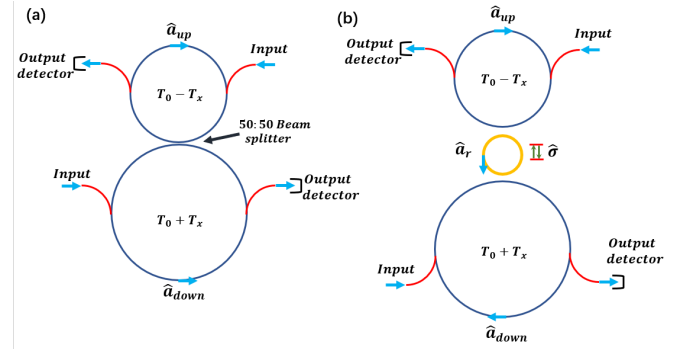


FIG. 4. (a) Implementing a quantum walk with linear 50/50 beam splitters using time-multiplexed synthetic dimensions. (b) Constructing a nonlinear quantum walk by replacing the 50/50 beam splitter with a single atom beam splitter. The single atom beam splitter consists of a two-level atom chirally coupled to the \hat{a}_r mode of a ring resonator (orange). In the “fast cavity regime” [34], the setup is equivalent to an atom coupled chirally to the two feedback loop modes, \hat{a}_{up} and \hat{a}_{down} .

Taking advantage of this idea, we propose the system shown in Figure 4b to implement the nonlinear Galton board. The beam splitter consists of an atom chirally coupled to the ring splitter mode \hat{a}_r [37–40]. The mode \hat{a}_r is then directionally coupled to the upper loop mode \hat{a}_{up} and lower loop mode \hat{a}_{down} . In the “fast cavity regime” [34, 35], one can adiabatically eliminate \hat{a}_r and hence the atom is chirally coupled to \hat{a}_{up} and \hat{a}_{down} with some effective decay rate [34]. The use of synthetic dimensions then enables us to build the nonlinear Galton board with this single device.

In summary, we have shown that an array of single

atom beam splitters can implement a strongly interacting two-photon quantum walk. By post-selecting photon detection events with certain time intervals, we can tune the output statistical pattern of the walk. Our quantum walk model can be easily generalized to more complicated quantum walks in higher dimensions or with nontrivial topology[10, 41–45]. Moreover, our formalism can be applied to a large family of light propagation problems consisting of feedforward networks with nonlinear input-output nodes. This broad family may include the n -photon scattering problem[24] or quantum neural networks[46]. Ultimately, our work can be extended in many ways and opens the door of a whole class of models with strong light-matter interactions for quantum simulation.

The authors would like to acknowledge financial support from the National Science Foundation (grant number OMA1936314 and ECCS1933546), the Air Force Office of Scientific Research (grant number UWSC12985 and FA23862014072), and the Army Research Laboratory (grant W911NF1920181).

* xzheng16@terpmail.umd.edu

† edowaks@umd.edu

- [1] A. M. Childs, R. Cleve, E. Deotto, E. Farhi, S. Gutmann, and D. A. Spielman, Exponential algorithmic speedup by a quantum walk, in *Conference Proceedings of the Annual ACM Symposium on Theory of Computing* (2003) pp. 59–68.
- [2] N. Shenvi, J. Kempe, and K. B. Whaley, Quantum random-walk search algorithm, *Physical Review A - Atomic, Molecular, and Optical Physics* **67**, 523071 (2003), [arXiv:0210064 \[quant-ph\]](#).
- [3] A. M. Childs, Universal computation by quantum walk, *Physical Review Letters* **102**, 1 (2009), [arXiv:0806.1972](#).
- [4] A. M. Childs, D. Gosset, and Z. Webb, Universal computation by multiparticle quantum walk, *Science* **339**, 791 (2013), [arXiv:1205.3782](#).
- [5] J. Kempe, Quantum random walks: An introductory overview, *Contemporary Physics* **44**, 307 (2003), [arXiv:0303081 \[quant-ph\]](#).
- [6] X. Qiang, Y. Wang, S. Xue, R. Ge, L. Chen, Y. Liu, A. Huang, X. Fu, P. Xu, T. Yi, F. Xu, M. Deng, J. B. Wang, J. D. Meinecke, J. C. Matthews, X. Cai, X. Yang, and J. Wu, Implementing graph-theoretic quantum algorithms on a silicon photonic quantum walk processor, *Science Advances* **7**, 1 (2021).
- [7] F. De Nicola, L. Sansoni, A. Crespi, R. Ramponi, R. Osellame, V. Giovannetti, R. Fazio, P. Mataloni, and F. Sciarrino, Quantum simulation of bosonic-fermionic noninteracting particles in disordered systems via a quantum walk, *Physical Review A - Atomic, Molecular, and Optical Physics* **89**, 32322 (2014), [arXiv:1312.5538](#).
- [8] L. Sansoni, F. Sciarrino, G. Vallone, P. Mataloni, A. Crespi, R. Ramponi, and R. Osellame, Two-particle bosonic-fermionic quantum walk via integrated photonics, *Physical Review Letters* **108**, 1 (2012), [arXiv:1106.5713](#).
- [9] M. A. Broome, A. Fedrizzi, B. P. Lanyon, I. Kassal, A. Aspuru-Guzik, and A. G. White, Discrete single-photon quantum walks with tunable decoherence, *Physical Review Letters* **104**, 1 (2010), [arXiv:1002.4923](#).
- [10] T. Kitagawa, M. A. Broome, A. Fedrizzi, M. S. Rudner, E. Berg, I. Kassal, A. Aspuru-Guzik, E. Demler, and A. G. White, Observation of topologically protected bound states in photonic quantum walks, *Nature Communications* **3**, 10.1038/ncomms1872 (2012).
- [11] K. Poullos, R. Keil, D. Fry, J. D. Meinecke, J. C. Matthews, A. Politi, M. Lobino, M. Gräfe, M. Heinrich, S. Nolte, A. Szameit, and J. L. O’Brien, Quantum walks of correlated photon pairs in two-dimensional waveguide arrays, *Physical Review Letters* **112**, 1 (2014), [arXiv:1308.2554](#).
- [12] H. Tang, C. Di Franco, Z. Y. Shi, T. S. He, Z. Feng, J. Gao, K. Sun, Z. M. Li, Z. Q. Jiao, T. Y. Wang, M. S. Kim, and X. M. Jin, Experimental quantum fast hitting on hexagonal graphs, *Nature Photonics* **12**, 754 (2018), [arXiv:1807.06625](#).
- [13] H. Tang, X. F. Lin, Z. Feng, J. Y. Chen, J. Gao, K. Sun, C. Y. Wang, P. C. Lai, X. Y. Xu, Y. Wang, L. F. Qiao, A. L. Yang, and X. M. Jin, Experimental two-dimensional quantum walk on a photonic chip, *Science Advances* **4**, 1 (2018), [arXiv:1704.08242](#).
- [14] A. M. Childs, D. Gosset, and Z. Webb, Universal computation by multiparticle quantum walk, *Science* **339**, 791 (2013), [arXiv:1205.3782](#).
- [15] A. A. Houck, H. E. Türeci, and J. Koch, On-chip quantum simulation with superconducting circuits, *Nature Physics* **8**, 292 (2012).
- [16] Z. Yan, Y. R. Zhang, M. Gong, Y. Wu, Y. Zheng, S. Li, C. Wang, F. Liang, J. Lin, Y. Xu, C. Guo, L. Sun, C. Z. Peng, K. Xia, H. Deng, H. Rong, J. Q. You, F. Nori, H. Fan, X. Zhu, and J. W. Pan, *Strongly correlated quantum walks with a 12-qubit superconducting processor* (2019).
- [17] M. T. Wong and C. K. Law, Two-polariton bound states in the Jaynes-Cummings-Hubbard model, *Physical Review A - Atomic, Molecular, and Optical Physics* **83**, 1 (2011).
- [18] X. Y. Sun, Q. H. Wang, and Z. J. Li, Interacting Two-Particle Discrete-Time Quantum Walk with Percolation, *International Journal of Theoretical Physics* **57**, 2485 (2018).
- [19] S. D. Berry and J. B. Wang, Two-particle quantum walks: Entanglement and graph isomorphism testing, *Physical Review A - Atomic, Molecular, and Optical Physics* **83**, 1 (2011).
- [20] A. Bisio, G. M. D’Ariano, N. Mosco, P. Perinotti, and A. Tosini, Solutions of a two-particle interacting quantum walk, *Entropy* **20**, 10.3390/e20060435 (2018), [arXiv:1804.08508](#).
- [21] J. T. Shen and S. Fan, Strongly correlated multiparticle transport in one dimension through a quantum impurity, *Physical Review A - Atomic, Molecular, and Optical Physics* **76**, 10.1103/PhysRevA.76.062709 (2007).
- [22] Y. Shen and J. T. Shen, Photonic-Fock-state scattering in a waveguide-QED system and their correlation functions, *Physical Review A - Atomic, Molecular, and Optical Physics* **92**, 1 (2015).
- [23] S. Xu, E. Rephaeli, and S. Fan, Analytic properties of two-photon scattering matrix in integrated quantum sys-

- tems determined by the cluster decomposition principle, *Physical Review Letters* **111**, 1 (2013).
- [24] S. Xu and S. Fan, Input-output formalism for few-photon transport: A systematic treatment beyond two photons, *Physical Review A - Atomic, Molecular, and Optical Physics* **91**, 1 (2015), arXiv:1502.06049.
- [25] O. Firstenberg, T. Peyronel, Q. Y. Liang, A. V. Gorshkov, M. D. Lukin, and V. Vuletić, Attractive photons in a quantum nonlinear medium, *Nature* **502**, 71 (2013).
- [26] Q. Y. Liang, A. V. Venkatramani, S. H. Cantu, T. L. Nicholson, M. J. Gullans, A. V. Gorshkov, J. D. Thompson, C. Chin, M. D. Lukin, and V. Vuletić, Observation of three-photon bound States in a quantum nonlinear medium, *Science* **359**, 783 (2018), arXiv:1709.01478.
- [27] H. Carmichael, *An Open Systems Approach to Quantum Optics, Lecture Notes in Physics m18* (1991) p. 147, arXiv:1211.6245.
- [28] H. J. Carmichael, Quantum trajectory theory for cascaded open systems, *Physical Review Letters* **70**, 2273 (1993).
- [29] A. Schreiber, K. N. Cassemiro, V. Potoček, A. Gábris, P. J. Mosley, E. Andersson, I. Jex, and C. Silberhorn, Photons walking the line: A quantum walk with adjustable coin operations, *Physical Review Letters* **104**, 1 (2010), arXiv:0910.2197.
- [30] A. Schreiber, K. N. Cassemiro, V. Potoček, A. Gábris, I. Jex, and C. H. Silberhorn, Decoherence and disorder in quantum walks: From ballistic spread to localization, *Physical Review Letters* **106**, 1 (2011), arXiv:1101.2638.
- [31] A. Schreiber, A. Gábris, P. P. Rohde, K. Laiho, M. Štefaňák, V. Potoček, C. Hamilton, I. Jex, and C. Silberhorn, A 2D quantum walk simulation of two-particle dynamics, *Science* **335**, 55 (2012), arXiv:1204.3555.
- [32] T. Nitsche, F. Elster, J. Novotný, A. Gábris, I. Jex, S. Barkhofen, and C. Silberhorn, Quantum walks with dynamical control: Graph engineering, initial state preparation and state transfer, *New Journal of Physics* **18**, 10.1088/1367-2630/18/6/063017 (2016), arXiv:1601.08204.
- [33] Y. Shikano, T. Wada, and J. Horikawa, Discrete-time quantum walk with feed-forward quantum coin, *Scientific Reports* **4**, 1 (2014).
- [34] S. Rosenblum, S. Parkins, and B. Dayan, Photon routing in cavity QED: Beyond the fundamental limit of photon blockade, *Physical Review A - Atomic, Molecular, and Optical Physics* **84**, 1 (2011), arXiv:1109.1197.
- [35] B. Dayan, a. S. Parkins, T. Aoki, E. P. Ostby, K. J. Vahala, and H. J. Kimble, A Photon Turnstile Dynamically Regulated by One Atom, *Science* **319**, 22 (2008).
- [36] T. Caneva, M. T. Manzoni, T. Shi, J. S. Douglas, J. I. Cirac, and D. E. Chang, Quantum dynamics of propagating photons with strong interactions: A generalized input-output formalism, *New Journal of Physics* **17**, 10.1088/1367-2630/17/11/113001 (2015), arXiv:1501.04427.
- [37] I. Söllner, S. Mahmoodian, S. L. Hansen, L. Midolo, A. Javadi, G. Kiršanske, T. Pregolato, H. El-Ella, E. H. Lee, J. D. Song, S. Stobbe, and P. Lodahl, Deterministic photon-emitter coupling in chiral photonic circuits, *Nature Nanotechnology* **10**, 775 (2015), arXiv:1406.4295.
- [38] P. Lodahl, S. Mahmoodian, S. Stobbe, A. Rauschenbeutel, P. Schneeweiss, J. Volz, H. Pichler, and P. Zoller, Chiral quantum optics, *Nature* **541**, 473 (2017), arXiv:1608.00446.
- [39] H. Pichler, T. Ramos, A. J. Daley, and P. Zoller, Quantum optics of chiral spin networks, *Physical Review A - Atomic, Molecular, and Optical Physics* **91**, 1 (2015), arXiv:1411.2963.
- [40] S. Mahmoodian, G. Calajó, D. E. Chang, K. Hammerer, and A. S. Sørensen, Dynamics of Many-Body Photon Bound States in Chiral Waveguide QED, *Physical Review X* **10**, 31011 (2020), arXiv:1910.05828.
- [41] T. Kitagawa, Topological phenomena in quantum walks: Elementary introduction to the physics of topological phases, *Quantum Information Processing* **11**, 1107 (2012), arXiv:1112.1882.
- [42] T. Kitagawa, M. S. Rudner, E. Berg, and E. Demler, Exploring topological phases with quantum walks, *Physical Review A - Atomic, Molecular, and Optical Physics* **82**, 10.1103/PhysRevA.82.033429 (2010), arXiv:1003.1729.
- [43] T. Kitagawa, E. Berg, M. Rudner, and E. Demler, Topological characterization of periodically driven quantum systems, *Physical Review B - Condensed Matter and Materials Physics* **82**, 1 (2010), arXiv:1010.6126.
- [44] S. Barkhofen, T. Nitsche, F. Elster, L. Lorz, A. Gábris, I. Jex, and C. Silberhorn, Measuring topological invariants in disordered discrete-time quantum walks, *Physical Review A* **96**, 1 (2017), arXiv:1606.00299.
- [45] C. Chen, X. Ding, J. Qin, Y. He, Y. H. Luo, M. C. Chen, C. Liu, X. L. Wang, W. J. Zhang, H. Li, L. X. You, Z. Wang, D. W. Wang, B. C. Sanders, C. Y. Lu, and J. W. Pan, Observation of Topologically Protected Edge States in a Photonic Two-Dimensional Quantum Walk, *Physical Review Letters* **121**, 1 (2018).
- [46] G. R. Steinbrecher, J. P. Olson, D. Englund, and J. Carolan, Quantum optical neural networks, *npj Quantum Information* **5**, 1 (2019), arXiv:1808.10047.

Supplementary Information: A strongly interacting photonic quantum walk using single atom beam splitters

I. METHOD AND FORMALISM

I.1. Derivation of input/output operators

We first derive the input/output operator at step n for arbitrary $n \leq N$ where N is the total number of steps. For a Galton board as shown below, we first define the following functions for site (n_1, x_1) and (n_2, x_2) :

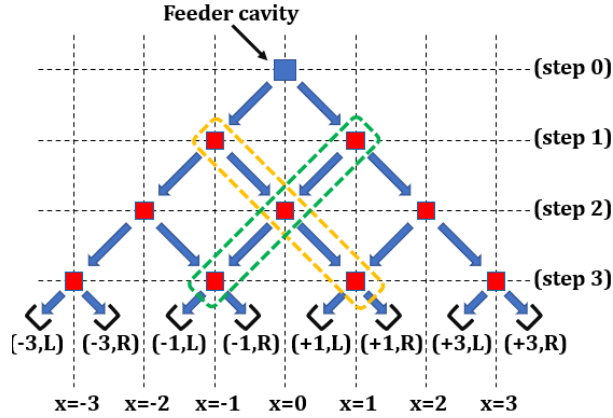


FIG. S1: A nonlinear Galton board with 3 steps. As an example, each pair of atoms in the green dashed box with $n_1 \neq n_2$ satisfies $\text{inline}(n_1, x_1; n_2, x_2) = -1$ whereas each pair in the orange dashed box with $n_1 \neq n_2$ satisfies $\text{inline}(n_1, x_1; n_2, x_2) = +1$.

$$\begin{aligned}
 \text{valid}(n_1, x_1) &= \begin{cases} 1, & \text{if } x_1 \equiv n_1 \pmod{2} \text{ and } |x_1| \leq n_1 \\ 0, & \text{else} \end{cases} \\
 \text{order}(n_1, x_1) &= n_1(n_1 + 1) + x_1 \\
 \text{inline}(n_1, x_1; n_2, x_2) &= \begin{cases} 1, & \text{if } n_1 - n_2 = x_1 - x_2, n_1 \neq n_2 \\ 0, & \text{else} \\ -1, & \text{if } n_1 - n_2 = x_2 - x_1, n_1 \neq n_2 \end{cases} \\
 \text{ift}(n_1, x_1; n_2, x_2) &= \begin{cases} 2, & \text{if } n_1 = x_1 = n_2 = x_2 = 0 \\ 1, & \text{else} \end{cases}
 \end{aligned} \tag{S1}$$

Intuitively, (n_1, x_1) is valid if such a site exist in a Galton board shown in (e.g. (1,-1) is valid but (1,0) is not). Any pair of labels (n, x) appearing in the equations below should satisfy $\text{valid}(n, x) = 1$. The order function labels the sites with unique integers from step 0 to step N . The inline function determines whether two sites are in the same line. Note that it yields $+1$ if (n_1, x_1) is on the top left of (n_2, x_2) and -1 otherwise, as shown in Figure S1. For simplicity, we define site operator $\hat{s}_{0,0} = \hat{b}_{0,0}$ and $\hat{s}_{n \neq 0, x} = \hat{\sigma}_{n, x}$. Similarly, the decay rate for each site is defined as $dr_{0,0} = \kappa$ and $dr_{n \neq 0, x} = \gamma$ where κ, γ are the decay rates of the cavity and atom, respectively. The ift function is introduced since $\hat{s}_{0,0}$ is bosonic, i.e. $|0, 0; 0, 0\rangle = \frac{1}{\sqrt{2}}(\hat{s}_{0,0}^\dagger)^2 |vac\rangle$. We can thus generally write

$$|n_1, x_1; n_2, x_2\rangle = \frac{1}{\sqrt{\text{ift}(n_1, x_1; n_2, x_2)}} \hat{s}_{n_1, x_1}^\dagger \hat{s}_{n_2, x_2}^\dagger |vac\rangle$$

Now we derive the input/output operator for arbitrary valid site (n_1, x_1) . The input/output relations can now be

written as:

$$\begin{aligned}\hat{a}_{n,x,L,out} &= \hat{a}_{n,x,R,in} + \sqrt{2dr_{n,x}}\hat{s}_{n,x} \\ \hat{a}_{n,x,R,out} &= \hat{a}_{n,x,L,in} + \sqrt{2dr_{n,x}}\hat{s}_{n,x}\end{aligned}\quad (\text{S2})$$

For all (n, x) such that $|n| = |x|$, we have the boundary condition:

$$\begin{aligned}\hat{a}_{0,0,L,in} &= \hat{a}_{0,0,R,in} = 0 \\ \hat{a}_{n,-n,L,in} &= \hat{a}_{n,n,R,in} = 0 \quad (\forall n \geq 1)\end{aligned}\quad (\text{S3})$$

Without loss of generality, we have the additional relations:

$$\begin{aligned}\hat{a}_{n,x,L,out} &= \hat{a}_{n+1,x-1,R,in} \\ \hat{a}_{n,x,R,out} &= \hat{a}_{n+1,x+1,L,in}\end{aligned}\quad (\text{S4})$$

By plugging in Equation S1 ~ S4, an arbitrary input/output operator can be written as:

$$\begin{aligned}\hat{a}_{n,x,L,in} &= \sum_{\substack{\text{inline}(n',x';n,x)=1 \\ \text{order}(n',x') < \text{order}(n,x)}} \sqrt{2dr_{n',x'}}\hat{s}_{n',x'} \\ \hat{a}_{n,x,R,in} &= \sum_{\substack{\text{inline}(n',x';n,x)=-1 \\ \text{order}(n',x') < \text{order}(n,x)}} \sqrt{2dr_{n',x'}}\hat{s}_{n',x'} \\ \hat{a}_{n,x,R,out} &= \sqrt{2dr_{n,x}}\hat{s}_{n,x} + \sum_{\substack{\text{inline}(n',x';n,x)=1 \\ \text{order}(n',x') < \text{order}(n,x)}} \sqrt{2dr_{n',x'}}\hat{s}_{n',x'} \\ \hat{a}_{n,x,L,out} &= \sqrt{2dr_{n,x}}\hat{s}_{n,x} + \sum_{\substack{\text{inline}(n',x';n,x)=-1 \\ \text{order}(n',x') < \text{order}(n,x)}} \sqrt{2dr_{n',x'}}\hat{s}_{n',x'}\end{aligned}\quad (\text{S5})$$

By plugging in $\hat{s}_{n,x}$ and $dr_{n,x}$, we get equation (4) in the manuscript as desired.

I.2. The effective Hamiltonian

Here we will use the result in section I.1 to find the effective Hamiltonian[1, 2]. We do this by induction, as shown in Figure S2.

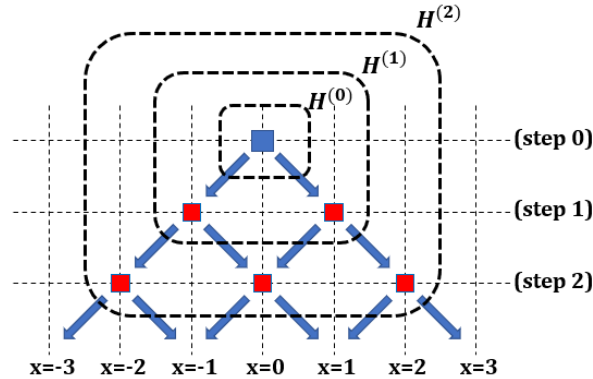


FIG. S2: $H^{(0)}$, $H^{(1)}$ and $H^{(2)}$ for a quantum Galton board.

In general, the Hamiltonian of the $n \geq 0$ step Galton board (i.e. $H^{(n)}$) drives the atoms at step $n+1$ with corresponding output operators, forming $H^{(n+1)}$. The case of $n = 0, 1, 2$ are shown in Figure S2. For $n = 0$, we get $H^{(0)} = -2i(\kappa + i\delta)\hat{b}_{0,0}^\dagger\hat{b}_{0,0}$ where κ is the feeder cavity decay rate and δ is the relative detuning between the feeder cavity and the atom. For any $n \geq 1$, we have:

$$H^{(n)} = H^{(n-1)} - i \sum_x \sqrt{2dr_{n,x}} \hat{s}_{n,x}^\dagger (\hat{a}_{n,x,L,in} + \hat{a}_{n,x,R,in}) - 2i \sum_x dr_{n,x} \hat{s}_{n,x}^\dagger \hat{s}_{n,x} \quad (S6)$$

Hence, by applying the above formula for $n = 1, 2, \dots, N$, we get the Hamiltonian for a quantum walk with N total steps:

$$H^{(n)} = -2i(dr_{0,0} + i\delta) \hat{s}_{0,0}^\dagger \hat{s}_{0,0} - i \sum_{1 \leq n \leq N, x} \sqrt{2dr_{n,x}} \hat{s}_{n,x}^\dagger (\hat{a}_{n,x,L,in} + \hat{a}_{n,x,R,in}) - 2i \sum_{1 \leq n \leq N, x} dr_{n,x} \hat{s}_{n,x}^\dagger \hat{s}_{n,x} \quad (S7)$$

By plugging in S5, we get an alternative form:

$$H^{(n)} = -2i(dr_{0,0} + i\delta) \hat{s}_{0,0}^\dagger \hat{s}_{0,0} - 2i \sum_{order(1,-1) \leq order(n,x) \leq order(N,N)} dr_{n,x} \hat{s}_{n,x}^\dagger \hat{s}_{n,x} - 2i \sum_{\substack{order(n',x') < order(n,x) \leq order(N,N) \\ |inline(n',x';n,x)|=1}} \sqrt{dr_{n',x'} dr_{n,x}} \hat{s}_{n,x}^\dagger \hat{s}_{n',x'} \quad (S8)$$

In summary, the Hamiltonian is a sum of terms of the form $-2i \times hc_{n',x';n,x} \hat{s}_{n,x}^\dagger \hat{s}_{n',x'}$ for $order(n,x) = order(n',x')$ or for $order(n',x') < order(n,x)$. The Hamiltonian coefficients $hc_{n',x';n,x}$ are given by $hc_{n',x';n,x} = \sqrt{dr_{n',x'} dr_{n,x}}$ except for $hc_{0,0;0,0} = \sqrt{dr_{0,0} dr_{0,0}} + i\delta$.

I.3. Solving the propagators

We are now ready to solve the dynamics of the system. Recall that in our quantum walk, the initial state of the system is $\frac{1}{\sqrt{2}}(\hat{b}_{0,0}^\dagger)^2 |vac\rangle = |0, 0; 0, 0\rangle$. The system first evolves for time t according to the equation $i \frac{d}{dt} |\psi\rangle = H^{(N)} |\psi\rangle$ until one photon is detected at one of the output channels. The system then collapses into a one excitation state and evolves for another time interval τ before the second photon is detected and the system goes back to $|vac\rangle$. Hence, we define two-photon-propagator $tpp_{n_1,x_1;n_2,x_2}(t)$ as follows:

$$tpp_{n_1,x_1;n_2,x_2}(t) = \langle n_1, x_1; n_2, x_2 | e^{-iH^{(N)}t} |0, 0; 0, 0\rangle \quad (S9)$$

And we require $order(n_1, x_1) \leq order(n_2, x_2)$ to avoid double counting. Hence, $tpp_{n_1,x_1;n_2,x_2}(t)$ represents the probability amplitude in front of the state vector $|n_1, x_1; n_2, x_2\rangle$ if we start with the initial state $|0, 0; 0, 0\rangle$ and evolve for time t .

We also need to define one-photon-propagator $opp_{n_1,x_1;n_2,x_2}(\tau)$:

$$opp_{n_1,x_1;n_2,x_2}(\tau) = \langle n_2, x_2 | e^{-iH^{(N)}\tau} |n_1, x_1\rangle \quad (S10)$$

Equivalently, $opp_{n_1,x_1;n_2,x_2}$ thus represents the probability amplitude, or complex value function in front of the basis vector $|n_2, x_2\rangle$ if we start with the initial state $|n_1, x_1\rangle$ and evolve it using the effective Hamiltonian for time τ .

We first demonstrate how to solve for all $opp_{n_1,x_1;n_2,x_2}(\tau)$. The differential equation for such propagator is:

$$\begin{aligned} \frac{d}{dt} opp_{n_1,x_1;n_2,x_2}(\tau) &= -(2hc_{n_2,x_2;n_2,x_2}) opp_{n_1,x_1;n_2,x_2}(\tau) \\ &- \sum_{\substack{valid(n_3-n_1,x_3-x_1)=1 \\ order(n_3,x_3) < order(n_2,x_2) \\ inline(n_3,x_3;n_2,x_2)=\pm 1}} (2hc_{n_3,x_3;n_2,x_2}) opp_{n_1,x_1;n_3,x_3} \end{aligned} \quad (S11)$$

For example, the "bottom layer" opp $opp_{0,0;2,0}$ would depend on the "top layer" opps: $\{opp_{0,0;1,-1}, opp_{0,0;1,1}\}$. These two opps would further be deduced from $opp_{0,0;0,0}(\tau) = e^{-(2\kappa+2i\delta)\tau}$. Likewise, $opp_{1,1;3,1}$ would depend on the set $\{opp_{1,1;2,0}, opp_{1,1;2,2}\}$. It should be noted that only $opp_{n_1,x_1;n_2,x_2}$ is non-zero only if (n_2, x_2) lies in the "light cone" of (n_1, x_1) as shown in Figure S3. Namely, we have $valid(n_2 - n_1, x_2 - x_1) = 1$.

From equation S11, one can see that $opp(n_1, x_1; n_1, x_1) = e^{-2hc_{n_1,x_1;n_1,x_1}\tau}$ and using induction, we can show that any opp has analytic solution of the form $F_1(t) = e^{-2\gamma\tau} p_1(\tau) + e^{-(2\kappa+2i\delta)\tau} p_2(\tau)$ where p_1, p_2 are some polynomials with finite order. We are then able to find the polynomial coefficients and hence the analytic solutions using induction.

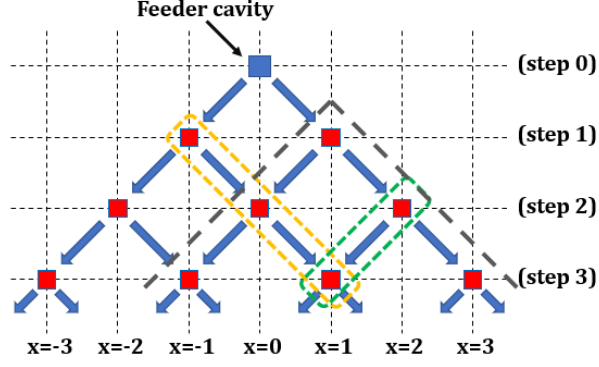


FIG. S3: The light cone in grey for site (1, 1). It should be notice that for site (3, 1), $opp_{1,1;3,1}$ would only rely on $opp_{1,1;n,x}$ for (n, x) in the light cone of (1, 1). Also, we must have $inline(n, x; 3, 1) = \pm 1$ and $order(n, x) < order(3, 1)$.

We now use two-photon version of the above method to find all tpps. The equation for a tpp is:

$$\begin{aligned}
\frac{d}{dt} tpp_{n_1, x_1; n_2, x_2}(t) &= -(2hc_{n_1, x_1; n_1, x_1} + 2hc_{n_2, x_2; n_2, x_2}) tpp_{n_1, x_1; n_2, x_2}(t) \\
&\quad - \sum_{\substack{inline(n_3, x_3; n_1, x_1) = \pm 1 \\ order(n_3, x_3) < order(n_1, x_1)}} (2hc_{n_3, x_3; n_1, x_1}) tpp_{n_3, x_3; n_2, x_2}(t) \\
&\quad - \sum_{\substack{valid(n_3 - n_1, x_3 - x_1) = 1 \\ order(n_1, x_1) < order(n_4, x_4) < order(n_2, x_2) \\ inline(n_4, x_4; n_2, x_2) = \pm 1}} (2hc_{n_4, x_4; n_2, x_2}) tpp_{n_1, x_1; n_4, x_4}(t) \\
&\quad - \sum_{\substack{valid(n_3 - n_1, x_3 - x_1) = 1 \\ order(n_4, x_4) \leq order(n_1, x_1) \\ inline(n_4, x_4; n_2, x_2) = \pm 1}} (2hc_{n_4, x_4; n_2, x_2}) tpp_{n_4, x_4; n_1, x_1}(t)
\end{aligned} \tag{S12}$$

One can see that except for $(0, 0; 0, 0)$, $tpp_{n_1, x_1; n_2, x_2} = 0$ for all $(n_1, x_1) = (n_2, x_2)$. Using a similar argument, we find that all tpp has the form $F_2(t) = e^{-4\gamma t} q_1(t) + e^{-(2\kappa + 2i\delta + 2\gamma)t} q_2(t) + e^{-(4\kappa + 4i\delta)t} q_3(t)$. Again, q_1, q_2, q_3 are polynomials with finite order.

Again, we can recursively find the polynomial coefficients and hence the analytic solutions, starting from $tpp_{0,0;0,0}(t) = e^{-(4\kappa + 4i\delta)t}$.

I.4. Computing correlations

Finally, we may obtain the correlations functions by combining opps with tpps. We start with the simpler correlations $\langle vac | \hat{s}_{n_2, x_2} e^{-iH\tau} \hat{s}_{n_1, x_1} e^{-iHt} | 0, 0; 0, 0 \rangle$, and note that:

$$\langle vac | \hat{s}_{n_1, x_1} e^{-iH\tau} \hat{s}_{n_2, x_2} e^{-iHt} | 0, 0; 0, 0 \rangle = \sum_{order(n_3, x_3) \leq order(n_2, x_2)} \sqrt{ift(n_3, x_3; n_2, x_2)} tpp_{n_3, x_3; n_2, x_2}(t) opp_{n_3, x_3; n_1, x_1}(\tau) \tag{S13}$$

Now the correlations we want are $\langle vac | \hat{a}_{1, out} e^{-iH\tau} \hat{a}_{2, out} e^{-iHt} | 0, 0; 0, 0 \rangle$ where $\hat{a}_{i, out}$ are output operators in equation S5 for $n = N$. These correlations are just linear combinations of the above correlations due to the relations in equation S5. Finally, we note that $\langle \hat{a}_{2, out}^\dagger(t) \hat{a}_{1, out}^\dagger(t + \tau) \hat{a}_{1, out}(t + \tau) \hat{a}_{2, out}(t) \rangle = |\langle vac | \hat{a}_{1, out} e^{-iH\tau} \hat{a}_{2, out} e^{-iHt} | 0, 0; 0, 0 \rangle|^2$. This allow us to obtain all $\Gamma_{1,2}(\tau, t)$.

I.5. Applying quantum trajectory theory to the linear quantum walk

Notably, the quantum trajectory theory approach can also be applied to study linear quantum walks. As mentioned in the main manuscript, the input/output relations for a linear, dispersionless beam splitter is given by:

$$\begin{aligned}\hat{a}_{n,x,L,out} &= r\hat{a}_{n,x,L,in} + t\hat{a}_{n,x,R,in} \\ \hat{a}_{n,x,R,out} &= t\hat{a}_{n,x,L,in} + r\hat{a}_{n,x,R,in}\end{aligned}\quad (\text{S14})$$

Here r is the reflection coefficient and t is the transmission coefficient satisfying $|r|^2 + |t|^2 = 1$. We construct a reference model by replacing all the single atom beam splitters with linear beam splitters with $r = \frac{-i\gamma}{i\gamma + \delta}$ and $t = \frac{\delta}{i\gamma + \delta}$ while keeping the same feeder cavity. Computationally, the non-Hermitian Hamiltonian is simply $\hat{H} = -2i(\kappa + i\delta)\hat{b}_{0,0}^\dagger\hat{b}_{0,0}$. The output operators at the final step are all proportional to $\hat{b}_{0,0}$ since $\hat{a}_{0,0,L,out} = \hat{a}_{0,0,R,out} = \sqrt{2\kappa}\hat{b}_{0,0}$ and the input-output relations are linear transformations(S14). For each output operator at the final step, we use S14 to obtain the correct complex coefficient in front of $\hat{b}_{0,0}$. We only have two non-zero tpp and opp : $tpp_{0,0,0,0}(t) = e^{-(4\kappa+4i\delta)t}$ and $opp_{0,0,0,0}(\tau) = e^{-(2\kappa+2i\delta)\tau}$. All the two photon correlation functions $\Gamma(\tau, t)$ are therefore proportional to $\sim e^{-4\kappa\tau}e^{-8\kappa t}$.

RESULTS

Case 1: $\gamma = \delta$

Here we present further results for $\kappa \ll \gamma = \delta$. In particular, we present the statistical patterns for the reference model (i.e. the non-interacting quantum walk with linear beam splitters). Indeed, as shown in Figure S4, the statistical pattern is τ -invariant.

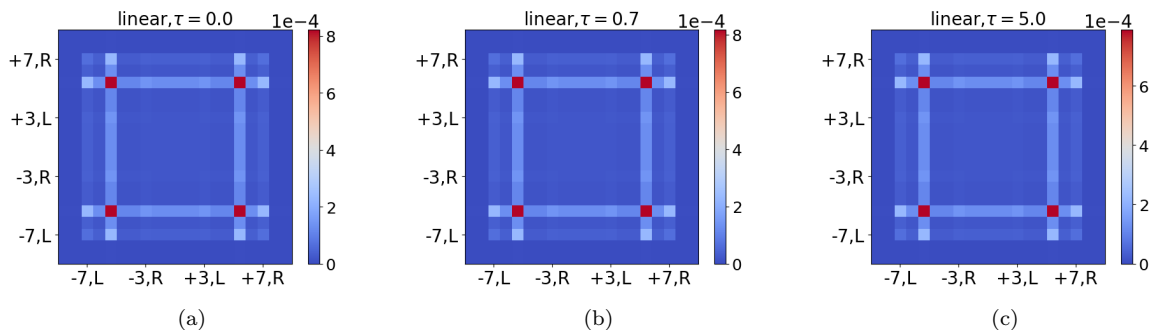


FIG. S4: τ -invariant statistical pattern of the linear quantum walk, for $\delta = \gamma$.

Case 2: $\delta = 0$

For the resonant case ($\delta = 0$), we see once again that the statistical pattern for the linear beam splitter quantum walk is τ -invariant(Figure S5). Furthermore, we pick two extra pairs of channels on the anti-correlated diagonal $(-3, L; +3, R); (+3, R; -3, L)$ and $(-1, L; +1, R); (+1, R; -1, L)$ and compare the interval-time correlation function $G(\tau)$ for all τ for both the linear and nonlinear quantum walk(Figure S6). These two pairs of channels exhibits similar correlation functions to that of the channel pair $(-5, L; +5, R); (+5, R; -5, L)$.

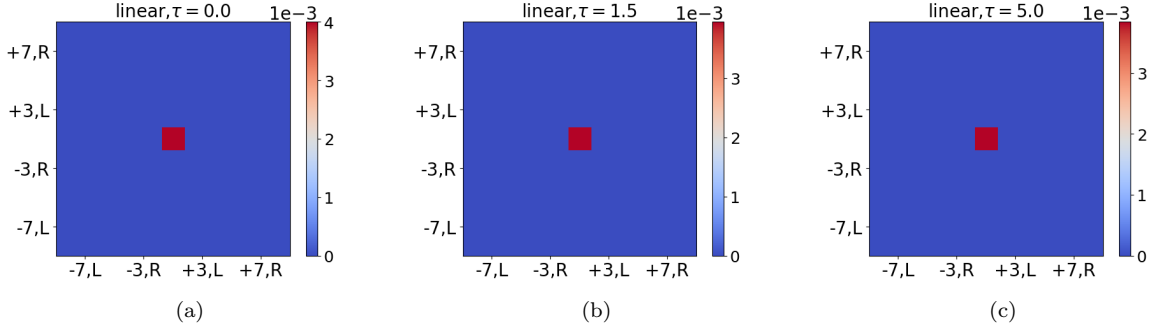


FIG. S5: τ -invariant statistical pattern of the linear quantum walk, for $\delta = 0$.

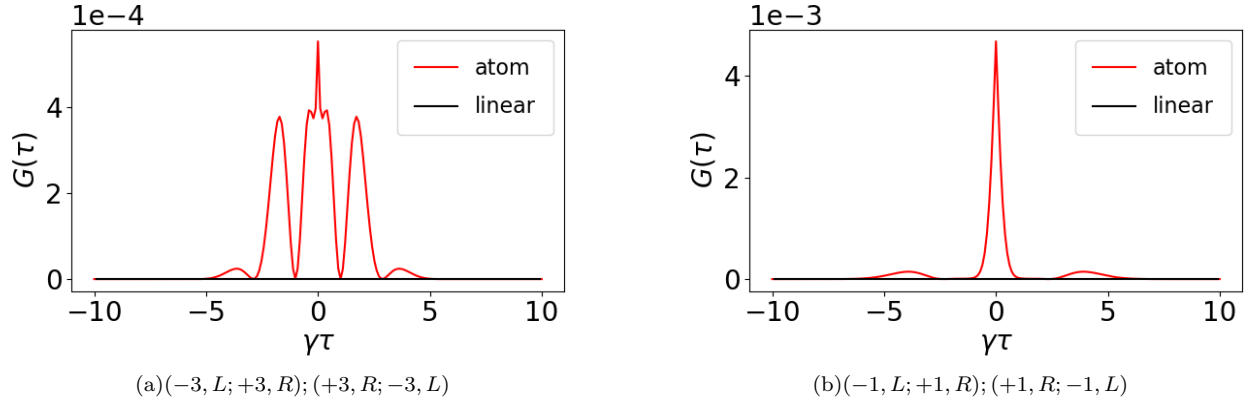


FIG. S6: Interval-time correlation functions $G(\tau)$ for two pairs of output channels on the anti-correlated diagonal. Note that the nature of correlation is similar to that of the channel pair $(-5, L; +5, R); (+5, R; -5, L)$ shown in the main manuscript.

-
- [1] H. Carmichael, *An Open Systems Approach to Quantum Optics, Lecture Notes in Physics m18* (1991), ISBN 3540566341, 1211.6245.
 [2] H. J. Carmichael, *Physical Review Letters* **70**, 2273 (1993), ISSN 00319007.